

# Improved wood–kirkwood detonation chemical kinetics

Kurt R. Glaesemann · Laurence E. Fried

Received: 17 November 2006 / Accepted: 12 February 2007 / Published online: 11 May 2007  
© Springer-Verlag 2007

**Abstract** We report an improved implementation of the Wood–Kirkwood kinetic detonation model based on a multi-species Buckingham exponential-6 equation of state (EOS) and multiple reaction rate laws. The exp-6 EOS allows for treatment of chemical systems at a statistical mechanics level, instead of an atomistic level. Finite global rate laws are used for the slowest chemical reactions. Other reactions are given infinite rates and are kept in constant thermodynamic equilibrium. The global rates do not necessarily correspond to a specific physical process, but rather to the sum total of slow physical processes. We model ideal and non-ideal composite energetic materials. We find that using the exp-6 non-ideal model improves the accuracy. The detonation velocity as a function of charge radius is also correctly reproduced.

**Keywords** Detonation · Kinetics · Explosive · Exponential-6

## 1 Introduction

The detonation of energetic materials is the result of the complicated relationship between chemistry and hydrodynamics. While the detailed chemical kinetics of detonation in gases has been studied extensively, much less is understood regarding chemical kinetic processes governing condensed energetic materials. The primary reason for this is the extreme

pressure (40 GPa) and temperature (4,000 K) immediately behind the detonation front. The extreme conditions result in very broad spectroscopic features that make the experimental identification of individual chemical species very difficult. Moreover, computational determination is also very difficult, with many species being meta-stable.

There is an ongoing need in the energetic materials field for reliable predictions of energy delivery and detonation velocity. Applications are wide and varied. This has conventionally been accomplished through the means of Chapman–Jouguet thermodynamic detonation theory. Chapman–Jouguet (C–J) Zel’dovich–von Neumann–Doering (ZND) detonation theory assumes that thermodynamic equilibrium of the detonation products is reached instantaneously. For C–J detonation, the Rayleigh line (describing conservation of momentum) intersects the shock Hugoniot (describing conservation of energy). The slope of the Rayleigh line is proportional to the detonation velocity, so that the C–J state is the slowest propagating state that can intersect the shock Hugoniot (and thus conserve energy). It should be noted that the Hugoniot is not a curve but a locus of end points.

For the purpose of this study we define non-ideal explosives as those with a reaction zone of 1 mm or more. So-called “non-ideal” explosives are often poorly modeled by Chapman–Jouguet theory, because these materials have chemical reaction rates that are slow compared to hydrodynamic time scale  $10^{-6}$  s so that the C–J assumption of instantaneous thermodynamic equilibrium is not valid. For example, it is found experimentally that the detonation velocity of non-ideal explosives varies sharply from the C–J value and depends strongly on the charge radius [1–3]. All explosives behave non-ideally if attempted to detonate on a small enough length scale. (i.e. The explosive runs out of material before it has time to reach a steady state.)

Contribution to the Mark S. Gordon on 65th Birthday Festschrift Issue.

K. R. Glaesemann (✉) · L. E. Fried  
Energetic Materials Center,  
Chemistry, Materials, and Life Sciences Directorate,  
Lawrence Livermore National Laboratory,  
L-282, P.O. BOX 808, Livermore, CA 94551-0808, USA  
e-mail: glaesemann1@llnl.gov

We are therefore forced to consider the interaction of chemical kinetics with the detonation wave in order to reach an acceptable representation of detonation in non-ideal explosives. Wood and Kirkwood [4] (WK) proposed a two-dimensional (2D) steady state kinetic detonation theory that solves many of the limitations of C–J theory. WK considered a cylindrical charge of infinite length. They solved the hydrodynamic Euler equations in the steady state limit along the central streamline of the cylinder. Radial expansion was treated as a source term in the 1D flow along the streamline.

Erpenbeck [5] extensively analyzed the WK equations. It is found that the detonation velocity depends on the interplay between chemical kinetics and radial expansion. In the limit of no radial expansion, the C–J plane wave result is obtained. When radial expansion is allowed; however, the detonation velocity can vary from the C–J prediction. In the limit of strong radial expansion the detonation wave fails; no velocity is found which satisfies the steady-state equations. Bdzil has generalized WK theory to off-axis flow [6] and Stewart and Yao [7] have studied the effect of kinetic rates on the decrease of detonation velocity with decreasing size and on curvature of the detonation wave.

In a previous work by Fried et al. [8] a model of detonation kinetics based on the identification of individual chemical species was implemented. The advantage of this treatment is that the same equations of state and chemical rate laws can be used on a wide range of explosive mixtures. A mixture equation of state based on thermal, mechanical, and partial chemical equilibrium is used. This mixture model is implemented in the Cheetah thermochemical code [9–11]. In the previous work by Fried et al., small molecules that are gases at standard conditions were treated with the BKW [12] real gas equation of state [13]. In the present work, a Buckingham exponential-6 equation of state (exp-6) is used to model small molecules [14, 15]. This equation of state has been found to be accurate over a wide range of pressures and temperatures. It is optimized for above the critical point and has a van der Waals loop below the critical point for some species, but these regions of phase space are not used during detonation processes. While WK theory successfully explained qualitative features of detonation, it has traditionally been applied only to the polytropic ideal gas equation of state (EOS). In condensed explosives, the adiabatic exponent varies from roughly three at the C–J state to roughly one after adiabatic expansion. Therefore, the polytropic EOS is inadequate to quantitatively model condensed explosives. Recently, we introduced a new version of our exp-6 EOS. The earlier version was considered a substantial update of the JCZ3 EOS, which was itself better than the ideal gas EOS. Not only were individual parameters improved, but also we moved from simple one-phase models to multi-phase models, often including multiple solid phases, for many species. These models are based on a combination

of diamond anvil cell data and shock data. We find that highly non-ideal explosives, such as ammonium perchlorate (AP), can be described with some success through the use of simple empirical reaction rate laws and a high-quality non-ideal EOS. Solids are treated with a Murnaghan [16, 17] equation of state. Simple pressure-dependent chemical reaction rates are employed. These rates represent the consumption of the energetic material by the detonation wave. Fast reaction rates (partial chemical equilibrium) are assumed for species other than the initial material.

The Wood–Kirkwood equations are solved numerically to find the steady-state detonation velocity. The radial expansion is derived from measured radii of curvature for the materials studied. We find good agreement with measured detonation velocities using the same set of equations of state and rate laws for each composite. Although our treatment of detonation is by no means exact, the ability to model a wide range of phenomena based on simple equations of state and rate laws is encouraging. We find that the inclusion of detonation kinetics yields a significant improvement in the predicted detonation velocity of materials with long estimated reaction zones. More importantly, we are able to reproduce the dependence of the detonation velocity on charge radius for several materials. For materials with short reaction zones, we recover the results of C–J thermochemistry.

## 2 WK detonation theory

Wood–Kirkwood theory starts with the hydrodynamic Euler equations coupled to chemical kinetics. The theory treats the detonation along the center of the cylinder. The Euler equations are reduced to their steady state form. The result is a set of ordinary differential equations that describe hydrodynamic variables and chemical concentrations along the center of the cylinder of explosive.

The reader is directed to Fried et al. [8] and Fickett and Davis [18] (see Eqs. 5.28, 5.37) for a complete discussion. We define  $\eta$  to be the *sonic parameter*. If the sonic parameter  $\eta$  is greater than zero communication with the shock front is possible. If it is less than zero the region cannot communicate with the shock front. Secondly, we will define the *pressure production* term  $\psi$ . Chemical reactions that increase the pressure at constant specific volume ( $v$ ) and energy ( $E$ ) will increase the value of  $\psi$ . Radial expansion, however, decreases the pressure ( $P$ ) and  $\psi$ .

## 3 Solution of the WK equations

The WK equations support a variety of solutions that have been discussed in great detail by Erpenbeck [5]. Let us consider the behavior of the equations as a function of the

specified detonation velocity  $D$ . There are three qualitatively different solutions possible. For special detonation velocities, the solutions pass through the sonic plane, defined by  $\eta = 0$ . Points behind the sonic plane cannot communicate with the shock front (i.e. The material is detonating and not simply burning very fast). The WK equations are finite when  $\eta = 0$  only if  $\psi$  also passes through zero. Therefore the sonic solutions are defined by the nonlinear equation  $\psi(t, D) = \eta(t, D) = 0$ . It is possible to think of this as the kinetic C–J condition. The next possibility is that  $\eta$  never passes through zero. These solutions are *overdriven*; that is the pressure increases with distance behind the shock front. These solutions correspond to a rear piston boundary condition that drives the shock front forward. Finally, if  $\eta = 0$  when  $\psi \neq 0$ , the equations become infinite. This means that a steady state flow cannot occur at the specified detonation velocity  $D$ . Of all the solutions generated by the WK equations, only the sonic solutions have the pressure tend to zero as  $t$  becomes large. It is these solutions that correspond to steady-state self-propagating flow.

#### 4 Mixture equation of state model

We now specify the equation of state used to model molecular mixtures. We treat the chemical equilibrium between  $N$  supercritical fluids or gaseous species and  $M$  condensed species. Liquids that are not supercritical are considered to be condensed phases. Condensed species  $i$  has  $C_i$  distinct phases. The Helmholtz free energy is a function of the system volume  $V$ , the temperature  $T$ , the molar concentrations of the fluid species  $x$  and the molar concentrations of the condensed species  $X$ . Since the gaseous and condensed species are assumed to be in separate phases, the Helmholtz free energy has the form:

$$A(x, X, V, T) = A^{\text{gas}}(x, V_g, T) + A^{\text{solid}}(X, V_c, T) \quad (1)$$

Here  $V_g$  is the volume of the gaseous phase and  $V_c$  is the volume of the condensed phase, so that  $V_g + V_c = V$ .

We now consider the condensed and gaseous contributions to the Helmholtz free energy separately. The gaseous free energy can be separated into an ideal gas contribution and an “excess” contribution:

$$A^{\text{gas}}(x, V, T) = A^{\text{ideal}}(x, V_g, T) + A^{\text{ex}}(x, V_g, T) \quad (2)$$

For the ideal gas portion of the Helmholtz free energy, we use a polyatomic model including electronic, vibrational, and rotational states. Such a model can be conveniently expressed in terms of the heat of formation, standard entropy, and constant pressure heat capacity  $C_p(T)$  of each species. The

excess portion of the free energy comes from a real gas equation of state.

We now turn to the condensed portion of the free energy. The  $i$ th condensed species has  $C_i$  condensed phases, which may possibly coexist in thermodynamic equilibrium. This yields the form:

$$A^{\text{solid}}(X, V_c, T) = \sum_i \sum_j X_{ij} A_{ij}(P, T) \quad (3)$$

with a summation over all species and phases. Here,  $X_{i,j}$  is the molar concentration of the  $j$ th phase of species  $i$ .  $A_{i,j}(P, T)$  is the molar free energy of the  $j$ th phase of species  $i$ .

The molar free energy  $A_{i,j}$  is expressed as a “reference” part at standard pressure, and a part due to pressure:

$$A_{ij}(P, T) = A_{ij}^0(T) + \Delta A_{ij}(P, T) \quad (4)$$

The reference part is determined through the JANNAF compilations of thermochemical data at standard pressure.  $\Delta A_{i,j}$  is determined by the condensed equation of state. We use a modified Murnaghan equation of state as follows:

$$V = V_0 [n\kappa P + \exp(-\alpha(T - T_0))]^{-1/n} \quad (5)$$

$V_0$  is the molar volume when  $P = 0$  and  $T = T_0$ .  $\kappa$  is the inverse of the isothermal bulk modulus.  $T_0$  is the temperature of the reference isotherm taken to be 298.15 K.  $\alpha$  is the volumetric coefficient of thermal expansion.  $n$  is the derivative  $dB(P, T)/dP$ , where  $B$  is the bulk modulus.

#### 5 Application to composite energetic materials

The detailed chemistry of composite energetic materials is very complex. Very many chemical steps are involved in the decomposition of most large energetic material molecules into small simple product molecules. In general the composition reactions are not well characterized, especially at elevated temperatures. The situation is made more complicated by the heterogeneous composite nature of most energetic materials. Void collapse and shear dislocations can lead to so-called “hot spots”—regions of enhanced temperature behind the detonation front. These regions play an essential role in high explosive initiation. They preclude describing the energetic material with a single temperature, and complicate the use of even the simplest Arrhenius chemical kinetic schemes.

Most reactive flow models of high explosive initiation overcome these difficulties through the use of pressure-dependent rates. Pressure-dependent rate laws have been shown to be sufficiently flexible to model a variety of initiation and non-ideal detonation phenomena, while maintaining simplicity. The disadvantage of these rate laws is that they

do not explicitly treat the high explosive microstructure or the underlying activated chemical reaction rate laws.

We have developed effective kinetic rates proportional to  $P^2$  for a variety of ideal and non-ideal explosives and their composites. We find that this choice, while simpler than most reactive flow rate laws for high explosive initiation, is adequate to model steady-state detonation over the range of materials and diameters provided here. We have made improvements to the empirical rates laws presented in Fried et al. [8], and these new rate laws fit a wider range of new experimental results. We are also studying the effect of treating a substantial portion of the aluminum present in aluminized explosives as an inert material. This is not only reasonable, but also essential because it is well known that not all aluminum reacts and some of the aluminum started as aluminum oxide.

We also predict sonic reaction zone widths. The sonic reaction zone width is the length of the zone behind the detonation front for which the local velocity of sound is equal to or greater than the detonation velocity. This zone is where chemical reactions contribute to the detonation wave. Beyond this zone, chemical reactions do not contribute the detonation wave.

For the purposes of this study, we model the kinetic processes of the high explosives as being a single decomposition reaction into primary product constituents. However, because we assume that all of the products are in thermochemical equilibrium, the results are independent of the assumed decomposition pathway. This would not be the case if irreversible reactions were important. Thus these rates are “global”, rather than a specific well-defined chemical process.

We assume that the kinetic rates are defined by the following equation:

$$\frac{d\lambda}{dt} = (1 - \lambda)RP^2 \quad (6)$$

where  $P$  is the pressure,  $R$  is the rate constant and  $\lambda$  represents the amount of unburned reactant normalized to vary between 0 (all unburned) and 1 (all burned). In our kinetics scheme the concentrations of reactants are assumed to be controlled by the kinetic rate, while all of the products are assumed to be in thermochemical equilibrium.

For non-ideal explosives, the effects of equations of state are strongly coupled to the effects of kinetics and hydrodynamics. For the equations of state, the usual process is to fit the covolumes of the product gases to experimental detonation velocities of ideal and non-ideal explosives. For this study we have used an EOS for gases *with parameters fit only to a wide range of experiments and a few first principle calculations*. The modified Murnaghan EOS was fit to shock Hugoniot and static data for individual product species.

## 6 Results

The explosives mixtures studied here are composed of HMX (1,3,5,7-tetranitroperhydro-1,3,5,7-tetrazocine,  $C_4H_8N_8O_8$ ), RDX (1,3,5-trinitroperhydro-1,3,5-triazine,  $C_3H_6N_6O_6$ ), PETN (1,3-dinitrato-2,2-bis (nitratomethyl) propane,  $C_5H_8N_4O_{12}$ ), and AP (ammonium perchlorate,  $NH_4ClO_4$ ), along with binder HTPB (hydroxyl-terminated polybutadiene,  $(C_4H_6)_aO_b$ ) and metal Al. In Fried et al.'s previous work, explosives with HTPB were all found to exhibit substantial non-ideal properties, and are presented in Table 1 [19]. That is, the experimental detonation velocity is significantly different than the calculated C–J theory detonation velocity. In modeling these composites, we assume that each component material burns at a rate (see Table 2), which is independent of the other components in the composite. We find that this simple approximation is adequate to describe the detonation velocity of the materials studied here. It should be noted that the approximation might fail for certain materials, most notably binary fuel/oxidizer mixtures, where the presence of one component dramatically accelerates the reaction of the other. The data for Table 3, as well as the experimental detonation velocities in Table 4, are taken from experimental results [1,2]. For all of the composites listed, there are experimentally determined radius of curvature measurements available to use as input to the WK calculation. The average absolute deviation from experimental values is also included in Table 4.

A summary of our results is presented in Table 4. There are notable deficiencies in the C–J detonation velocity calculations when compared to experiment. In Fig. 1 we compare

**Table 1** Non-ideal composites

Composite	Composition by weight
PBXN-110	HMX, 88%, HTPB, 12%
PBXN-111	RDX, 20%, AP, 43%, Al, 25%, HTPB, 12%
IRX1	HMX, 70.1%, HTPB, 29.9%
IRX-3A	HMX, 69.8%, Al, 10%, HTPB, 20.2%
IRX4	HMX, 30%, AP, 24%, Al, 16%, HTPB, 30%

**Table 2** Effective chemical reactions controlled by kinetics

Reactant	Products	$R \mu s^{-1} GPA^{-2}$
Al, O <sub>2</sub>	Al <sub>2</sub> O <sub>3</sub>	0.0075
AP	N <sub>2</sub> , H <sub>2</sub> O, O <sub>2</sub> , HCl	0.0075
HMX	CO <sub>2</sub> , H <sub>2</sub> , N <sub>2</sub>	0.2000
HTPB	C, CH <sub>4</sub> , H <sub>2</sub> O	0.0010
RDX	CO <sub>2</sub> , H <sub>2</sub> O, n <sub>2</sub> , O <sub>2</sub> , C	0.2000

**Table 3** Density  $\rho$ , charge radius  $R_0$ , and radius of curvature  $R_c$  of composite energetic materials studied here

Composite	$\rho$ (g/cc)	$R_0$ (mm)	$R_c$ (mm)
PBXN-110	1.680	24.95	245.10
PBXN-111(1)	1.790	12.60	51.90
PBXN-111(2)	1.790	18.95	107.40
PBXN-111(3)	1.790	23.49	143.30
PBXN-111(4)	1.790	50.00	479.80
IRX-1	1.430	25.00	206.61
IRX-3A	1.580	25.00	177.30
IRX-4	1.500	25.00	130.55

**Table 4** Calculated detonation velocities in km/s with C–J theory (C–J), experimental detonation velocities (EXP), previous Fried et al. [8] results (OLD), and exp-6 WK (WK). Reaction zones (RZ) are calculated with WK

Material	C–J	EXP	OLD	WK	RZ (mm)
PBXN-110	7.78	8.39	8.37	8.36	0.21
PBXN-111(1)	6.91	5.13	4.78	4.80	1.18
PBXN-111(2)	6.91	5.41	5.44	5.39	2.25
PBXN-111(3)	6.91	5.51	5.62	5.55	2.02
PBXN-111(4)	6.91	5.75	5.97	5.80	1.80
IRX1	6.93	7.49	7.10	7.45	0.36
IRX-3A	7.17	7.79	7.30	7.54	0.35
IRX4	6.60	5.62	4.98	5.22	1.44
Deviation from EXP values	1.08	0.00	0.28	0.15	N/A

detonation velocities calculated with C–J theory to experimental values.

In Fig. 2 we plot detonation velocities obtained with WK detonation theory and the reactions. The kinetic calculations are nearly as accurate at detonation velocities. Although the calculations are not exact, all the large deviations from experiment have been eliminated or reduced.

Figures 3 and 4 show our results for PBXN-111. The open diamonds are the experimental detonation velocity as a function of radius from Forbes and Lemar [20], while the solid diamonds are our calculated values. Our calculated values reproduce the experimental values reasonably well, while using generic kinetic rates given in Table 2 (with the noticeable exception of the smallest explosive charge). The shape of the curve, however, is sensitive to the rates chosen for AP and Al. In addition, for we find multi-valued solutions for the detonation velocity. In such a case we take the smallest figure of merit. The solution of the WK equations is complicated from a numerical point of view, since the WK equations will become singular. We have found it most robust to transform the root search problem into a minimization. We define a

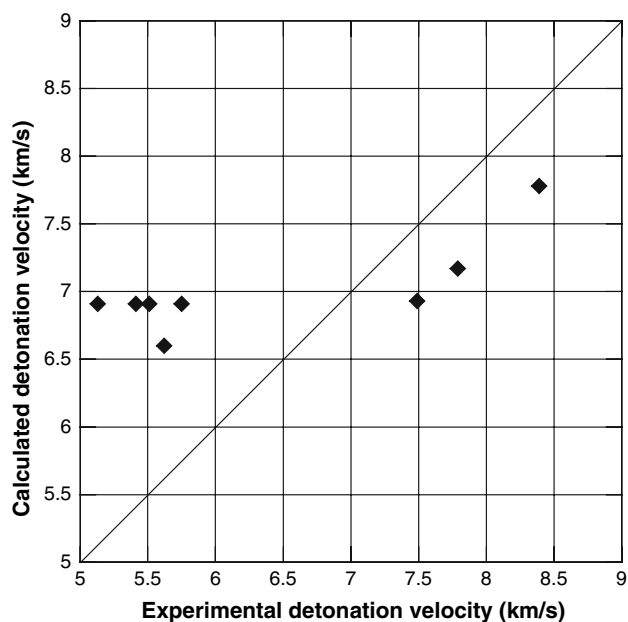
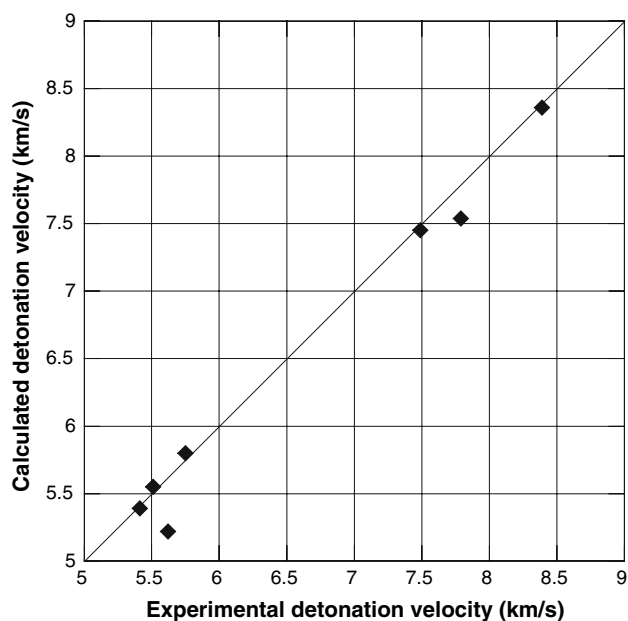
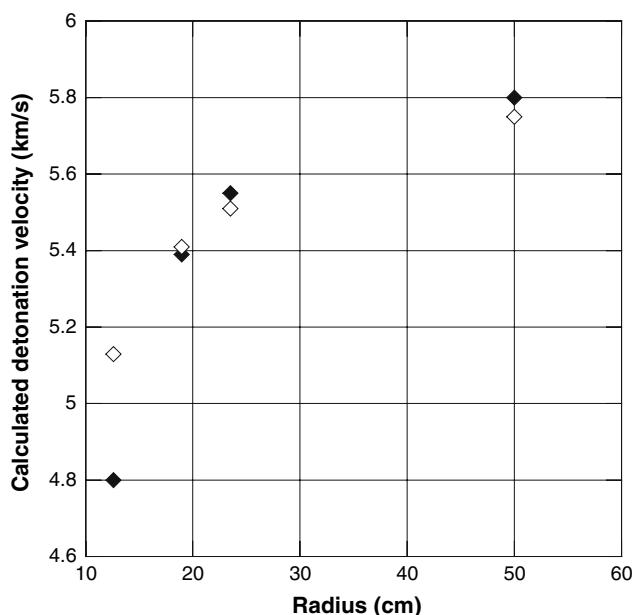
**Fig. 1** Detonation velocities (in km/s) as calculated with C–J theory and the exp-6 EOS**Fig. 2** Detonation velocities (in km/s) as calculated with WK theory and the exp-6 EOS

figure of merit function to be:

$$Y(D) = \min_{0 < t < t_{\max}} \eta^2 + t^2 \psi^2 \quad (7)$$

We have  $Y = 0$  when the detonation is successful. We have multiplied  $\psi$  by  $t$  to yield a unitless function that works equally well for fast or slow reaction rates.  $t_{\max}$  is set to be longer than chemical reaction timescales. If a singular solution is encountered ( $\eta$  goes to zero when  $\psi$  is nonzero),



**Fig. 3** WK theory predicts the detonation velocity as a function of size for PBXN-111. *Open diamonds* are experimental values

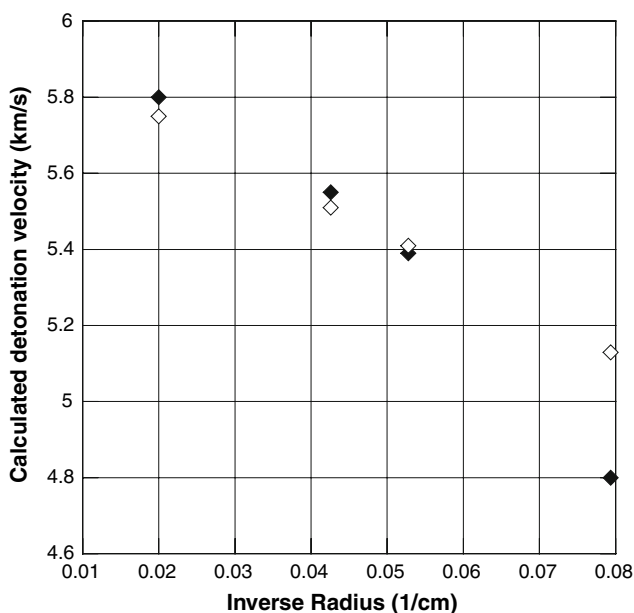


**Fig. 4** WK theory predicts the detonation velocity as a function of inverse size for PBXN-111. *Open diamonds* are experimental values

then  $t_{\max}$  is taken to be the time at which the singularity occurs.

Kennedy and Jones [21] have previously studied the non-ideal behavior of PBXN-111. Experiments with PBXN-111 have been performed from a charge radius of 50 cm, down to the failure radius which is less than 9.5 cm. Previous estimates of the equilibrium C–J detonation velocity of PBXN-111 by Kennedy and Jones range from 6.75 to 8.00 km/s. Our estimate of the equilibrium C–J detonation velocity of

PBXN-111 is 6.91 km/s. A significant difference between our calculations and previous ones is that with our carbon equation of state we predict all of the carbon is in the gas state at the C–J point, while Kennedy and Jones predict a significant amount of diamond is produced at C–J.

In conclusion, we have developed a kinetic model for thermochemical detonations based on Wood–Kirkwood theory and the thermochemical Cheetah code. We find that with a simple model for kinetic processes we are able to model many of the features of non-ideal explosives such as their detonation velocities and their sonic reaction zone widths. In the future, we plan to extend our kinetic modeling study to include temperature and pressure dependent rate laws. In this way we can extend our model to more physically based rate laws and study more complex non-ideal detonation behavior such as shock initiation, hot spot formation and failure processes.

**Acknowledgments** This work was performed under the auspices of the U.S. Department of Energy by the Lawrence Livermore National Laboratory under contract No.-W-7405-48. This work is supported by the Joint DoD/DOE Munitions Technology Development Program, a program funded by the Department of Defense and the Department of Energy. This work is supported by The Advanced Simulation and Computing Program (ASC), which is the National Nuclear Security Administration (NNSA) collaborative program among Lawrence Livermore, Los Alamos, and Sandia national laboratories to ensure the safety and reliability of the nation's nuclear weapons stockpile.

## References

1. Marsh SP (1980) LASL Shock Hugoniot Data. University of California Press, Berkeley
2. Dobratz BM, Crawford PC (1985) LLNL Explosives handbook properties of chemical explosives and explosive simulants, report UCRL-52997 change 2, 31 January 1985, LLNL, Livermore, CA
3. Souers PC (1998) A library of prompt detonation reaction zone data, Lawrence Livermore National Laboratory Report, UCRL-ID-130055, Rev. 1 June 1998, LLNL, Livermore, CA
4. Wood WW, Kirkwood JG (1954) J Chem Phys 22:1920–1924
5. Erpenbeck JJ (1964) Phys Fluids 7:684–696
6. Bdzil JB (1981) Fluid Mech 108:195–206
7. Stewart DS, Yao J (1998) Combust Flame 113:224–235
8. Howard WM, Fried LE, Souers PC (2000) In: Proceedings of the 11th international detonation symposium, Snowmass CO, 31 August–4 September 1998, pp 998–1006
9. Fried LE, Howard WM, Souers PC (1998) CHEETAH 2.0 user's manual, Lawrence Livermore National Laboratory Report UCRL-MA-117541 Rev. 5, 1998, LLNL, Livermore, CA
10. Fried LE, Glaesemann KR, Howard WM, Souers PC, Vitello PA (2004) Lawrence Livermore National Laboratory. UCRL-CODE-155944
11. Fried LE, Glaesemann KR, Howard WM, Souers PC, Vitello PA (2007) Lawrence Livermore National Laboratory. Cheetah 5.0 is in final development
12. Fried LE, Souers PC (1996) Propellants Explosives Pyrotechnics 21:215–223

13. Hobbs ML, Baer MR (1995) In: Proceedings of the 10th international detonation symposium, Boston, MA, 12–16 July 1993, pp 409–418
14. Fried LE, Howard WM (1998) *J Chem Phys* 109:7338–7348
15. Glaesemann KR, Fried LE (2007) In: Proceedings of the 13th international detonation symposium, Norfolk, VA, 23–28 July 2006 (in press)
16. Fried LE, Howard WM (2000) *Phys Rev B* 61:8734–8743
17. Murnaghan FD (1944) *Proc Natl Acad Sci (USA)* 30:244–247
18. Fickett W, Davis WC (1979) *Detonation*, chap 5. University of California Press, Berkeley
19. Sutherland GT, Brousard LJ, Leahy JF, Prickett S, Deiter JS (2004) *J Energ Mater* 22:181–197
20. Forbes JW, Lemar ER (1998) *J Appl Phys* 84:6600–6605
21. Kennedy DL, Jones DA (1995) In: Proceeding of the 10th international detonation symposium, Boston Massachusetts, 12–16 July 1993, pp 665–674